SAND2019-14611J

Array directivity enhancement by leveraging angle-dependent scattering

Dagny Joffre

University of Massachusetts – Lowell / Sandia National Laboratories*

1 University Ave

Lowell, MA 01854

Dagny_joffre@student.uml.edu

Christopher Niezrecki, Peter Avitabile

University of Massachusetts – Lowell

1 University Ave

Lowell, MA 01854

Christopher_Niezrecki@uml.edu, Peter_Avitabile@uml.edu

Manuscript submitted: 8 July 2019

Running Title: Enhanced Sonar Directivity

Sandia National Laboratories is a multimission laboratory managed and operated by National Technology & Engineering Solutions of Sandia, LLC, a wholly owned subsidiary of Honeywell International Inc., for the U.S. Department of Energy's National Nuclear Security Administration under contract DE-NA0003525.

Abstract

The quality of a sonar array's localization capabilities, often expressed as directivity, is limited by the sonar's aperture, that is, the length of the sonar array. Previous attempts to improve directivity, without increasing array size, have been moderately successful. Wave scattering within a nontraditional array, such as an array fabricated from a non-homogenous material, could provide additional information to the localization calculations and improve array directivity without increasing the size of the array. An investigation of array directivity improvement through wave scattering is performed. This paper modifies existing localization and directivity calculations to consider the scattered waves, and uses the derived equations to explain why previous proposed scattering was incapable of increasing directivity. A scattering relationship capable of enhancing array localization without increasing array size is proposed, and the directivity improvement claims are verified with beamform plot comparisons and directivity index calculations.

Keywords: Directivity, Bragg scattering, Localization, Array

I. Introduction

One major limitation to array localization is the array aperture, in which larger arrays produce more precise location estimations and are more resistant to the influences of noise[1]. An array's localization capability can be quantified as the directivity of the array, in which high directivities are desired and traditionally achieved through the use of larger arrays. Although large arrays are desired, they are often infeasible to implement due to the cost and the physical space available[2].

Several methods have been investigated in an attempt to improve directivity without expanding the array size. These methods include weighting optimization[3-5], synthetic expansion[6-8], and internal scattering[9,10]. The most common method of enhancing an array's measurement without requiring longer arrays is the use of weighting optimization, which is applied during the beamforming process.

Arrays excited by acoustic plane waves respond at wavenumbers within the acoustic cone from □ω/c to ω/c, where ω is the excitation frequency and c is the speed of sound in the underwater environment. Traditionally, arrays are designed to operate within the acoustic cone, and responses beyond this are often considered unwanted noise. Beamforming algorithms, such as Delay-and-Sum (DAS), steer among the known response wavenumber region to calculate a beamform plot. Equations 1 and 2 are commonly used to perform the DAS calculation[3]. Equation 1 writes the beamform plot value, B, as a function of steering angle, θ_s, in which the sensor measurement of the transverse response, y_n, is multiplied by a weight, w_n, and a term accounting for the phase delay in sensor responses as the excitation propagates down the array, τ_n. The phase delay term for the chosen steering angle is applied to all sensors, and then summed over all sensors and over all time. Beamform plots are generated by calculating beamform values for the full region of potential excitation angles. Note that a beamform plot is a function of the steering angle because the actual incident angle is unknown. For a one-dimensional baffled array, such as an array attached to the side of a ship or submarine, the steering angles would range from □90° to 90°. Equation 2 defines the phase delay, in which x_n is the location of the measurement sensor in the array and x_{ref} is a reference position for the array sensors. The first portion of the phase delay term, the steering wavenumber, describes the wavenumber of a plane wave located at the steering angle. When the reference sensor location is zero the phase delay can be rewritten as simply the steering wavenumber, $k(\theta_s)$, multiplied by the sensor location, as in Equation 2.

$$B(\theta_s) = \sum_{t=0}^{T} \sum_{n=0}^{N-1} w_n y_n(t) e^{-i\tau_n(\theta_s)} \quad (1)$$

$$\tau_n = \frac{\omega}{c} \sin(\theta_s)\left(x_n - x_{ref}\right) = k(\theta_s) x_n \quad (2)$$

Examples of the resulting beamform plots of a 1 kHz excitation in air (c = 343 m/s) at □30° on linear, one-dimensional, 1.82 m and 3.64 m-long homogenous arrays are shown in Figure 1. Excitation in air was used to remain consistent with experimental testing not discussed in this paper, and to produce narrower main lobes which better illustrate the following discussion. Excitation in water may be simulated by changing the speed of sound value. The main lobes are compared, in which the array with a higher directivity (the 3.64 m array) produces a beamform plot with a narrower main lobe.

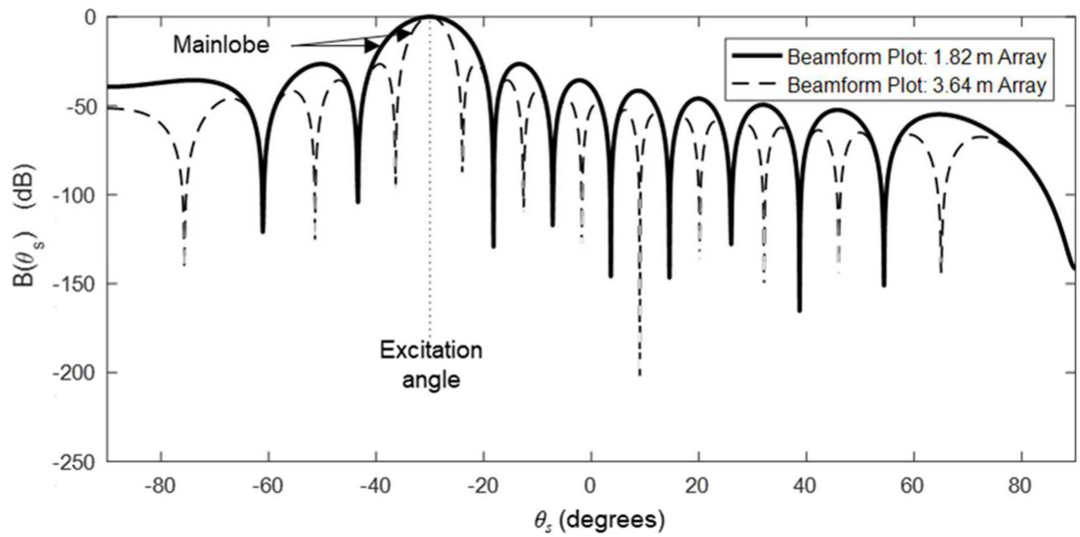

Fig. 1. Comparison of beamform plot main lobes for a 1.82 m array (solid line) and a 3.64 m array (dashed line) from a 1 kHz plane wave excitation in air at □30°.

The weighting term in Equation 1 can improve the beamform plot if appropriate weights are chosen. Optimization methods have been defined to choose the best weighting terms, such as Minimum Variance Distortionless Response (MVDR)[4,5], has been shown to be very effective at improving localization. However, it is important to realize that weighting optimization techniques do not increase the directivity of the array, they only improve the localization calculation from the measurements available. If optimized weighting could be applied to measurements from an array with higher directivity, the resulting localization will be even better.

Synthetic expansion[6-8] is another method used to improve the directivity of an array. Synthetic expansion uses the motion of the array vehicle (such as a ship or submarine) to take measurements across a large area, and then stitches all measurements together before beamforming. The resulting data spans an area much longer than the actual array, and a higher directivity is achieved. Synthetic apertures were initially proposed by Yen[6], but thoroughly studied by Stergiopolous[7,8]. Although the method was successful in improving array directivity, it also constrained the motion of the vehicle and required substantial processing power.

One more proposed improvement technique leverages internal wave scattering induced when a nonhomogeneous array material is used. Wave propagation within a nonhomogeneous array introduces additional scattered waves that contain information about the location of the incident acoustic signal, similar to the waves formed in a traditional homogeneous array. However, the scattered waves will have a smaller wavelength than the traditional waves, and additional information may be extracted from the scattered waves about the origin of the acoustic signal. The idea of scattering as a method of directivity improvement was first proposed by Cray[9,10]. Cray theorized improved directivity based on the decreased wavelength of scattered signals, and analyzed the scattering in a non-homogenous array consisting of periodic aluminum ribs in a urethane hull-mounted array to generate Bragg scattered waves.

Periodically ribbed materials capable of manipulating acoustic signals through Bragg scattering, such as Cray's proposed array design, is a form of a phononic crystal[11]. These materials are typically investigated for the generation of a band gap; a narrow frequency region in which only evanescent waves exist, and therefore no wave propagation exists. The waves in a band gap have the potential to respond in unique ways, and studies have applied band gaps to lens focusing[12], signal reduction[13], waveguides[14], and cloaking[15]. A review paper on applications of phononic crystals has recently been published[16] and Elachi[17] provides a lengthy compendium on Bragg scattering effects in periodic structures, yet within the previous body of literature, Cray is the only author that this work's authors are aware of to consider the use of a phononic crystal as a broadband localization improvement technique.

The wavenumbers of Bragg scatted waves (called Bragg replicates) are predicted using Equation 3, in which the wavenumber, $k_n(\theta)$, is written as a function of excitation frequency, ω, environmental speed of sound, c, and incident angle, θ, plus a replicate term defined by the periodicity, a, and an integer multiple, n, that defines the predicted replicate[18]. For example, if the integer multiple is 0, the wavenumber is the original wavenumber that would manifest in a homogenous panel. If the integer multiple is □1, then the wavenumber is predicted for the first negative replicate.

$$k_n(\theta) = \frac{\omega}{c}\sin(\theta) + \frac{2\pi}{a}n \tag{3}$$

The spatial and wavenumber responses of traditional arrays are shown in Figures 2a and 2b, and are compared to the spatial and wavenumber responses of periodic sonar arrays that Bragg scatter the incident waves, shown in Figures 2c and 2d, respectively.

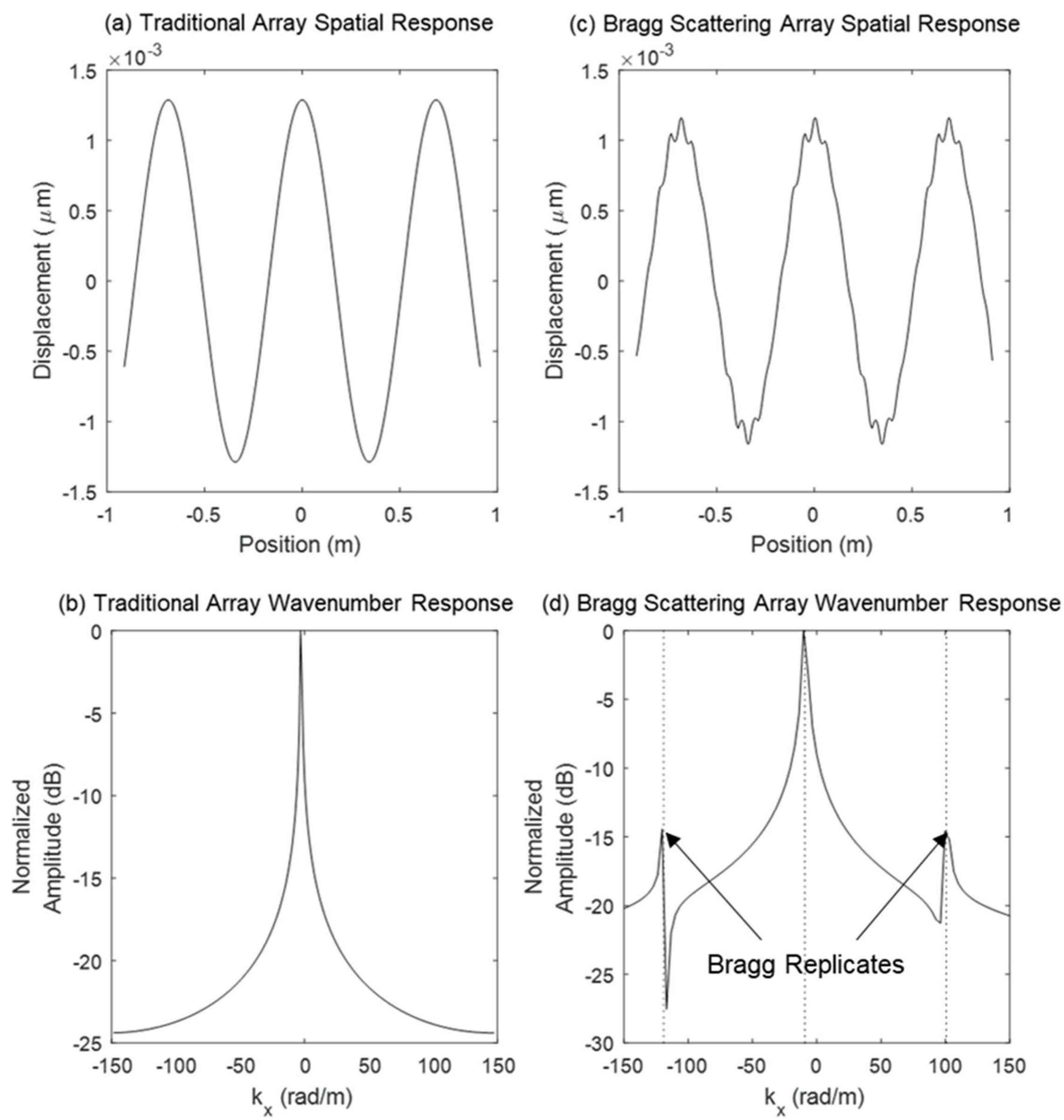

Fig. 2. Array response to a 1 kHz excitation in air at □30° for a traditional, pure urethane array in the (a) spatial (displacement) domain and (b) wavenumber domain, and the response to the same excitation for a ribbed array in the (c) spatial (displacement) domain and (d) wavenumber domain.

Cray reasoned that the Bragg replicates should result in higher directivities because the replicate wavelengths were smaller than the traditional wavelengths (the ratio of the number of replicate wavelengths to the fixed array aperture increases, thus increasing directivity). However, Cray later redacted this claim, stating that array directivity enhancement could not be obtained from the reduced wavelength of the Bragg replicate waves[19].

This paper will explain why fixed periodic Bragg replicates are incapable of improving directivity, and will introduce the scattering behavior that is required of a nonhomogeneous array to achieve enhanced directivity. If successfully designed, signal scattering as an array enhancement method could be a promising method of passive directivity improvement. Wave scattering would inherently improve directivity, would not depend on the movement of the vessel, and would not increase the computational load for localization estimation. Directivity improvement claims are supported with beamform plots and directivity index comparisons between traditional arrays and the proposed scattering array. The definition of a wave scattering relationship capable of enhancing array directivity is the first step towards array performance improvement without the need to increase array size.

II. Scattered wave beamforming and directivity equations

Scattered waves lay in a different region in the wavenumber domain than the waves used in traditional beamforming. The DAS equations need to be rewritten to consider the appropriate wavenumber region before scattered waves can be used to estimate the location of the acoustic excitation. The wavenumber region of interest is modified from traditional waves to scattered waves by substituting the traditional phase delay, τ_n, with the scattered phase delay, τs_n, defined in Equation 4, in which $k_s(\theta_s)$ is the predicted wavenumber of the scattered wave at the chosen steering wavenumber, θ_s[10].

$$\tau s_n = k_s(\theta_s) x_n \tag{4}$$

The resulting beamform plots can indicate if the scattered waves will improve the directivity of the array. If the main lobe of the beamform plot calculated from the scattered waves is narrower than the main lobe of the beamform plot, and the sidelobes levels are equivalent, calculated from a traditional array of the same size, then the scattered waves will improve the directivity of the array.

The main lobe of the beamform plot is an indicator that directivity is improved, but it is not a definite determination of directivity change. Optimized weighting algorithms, for example, significantly decrease the main lobe in beamform plots, but at a cost of raising sidelobe levels, and hence have no effect on the array directivity. Therefore the directivity of the array must also be calculated to show that scattered waves can inherently improve an array's directivity.

The directivity of an array can be quantified by calculating the directivity index (DI) for a particular incident angle. The DI describes an array's ability to suppress a diffuse noise field, in which a higher DI indicates an array is more adept at suppressing noise[20]. The noise suppression capability manifests as a narrower main lobe in a beamform plot. The DI equation for traditional arrays is written in Equation 5 as a function of an angular response term, A, in a form similar to that used in Lee[21], but for a one-dimensional array with uniformly spaced sensors and uniform weighting. These assumptions allow for significant simplifications to the angular response equation. Equation 6 defines the angular response term as a function of the difference between the actual incident wavenumber, $k(\theta)$, and the steering wavenumber, $k(\theta_s)$, assuming constant sensor spacing and uniform sensor directivity.

$$DI(\theta) = 10\log_{10}\left(\frac{2N^2}{\int_{-\frac{\pi}{2}}^{\frac{\pi}{2}} |A(\theta)|^2 \cos(\theta)\, d\theta}\right) \tag{5}$$

$$A(\theta) = \sum_{n=1}^{N} e^{i\left(k(\theta)-k(\theta_s)\right)x_n} \tag{6}$$

Consider the angular response term in Equation 5. For DI to increase, the integral in the denominator must decrease. The integral decreases when the exponential term in Equation 6 becomes narrower in angle. For traditional arrays, the wavenumber term is written in the form $(\omega/c)\square\sin(\theta)$ for the excitation wavenumber and $(\omega/c)\square\sin(\theta_s)$ for the steering wavenumber. By increasing frequency (ω), decreasing wave speed in the environment (c), or increasing the length of the array (x_n), the exponent term can be increased, therefore increasing the DI.

The DI calculation was modified for scattered waves by substituting the traditional wavenumber terms in the angular response equation ($k(\theta)$ and $k(\theta_s)$) with the scattered wavenumber terms ($k_s(\theta)$ and $k_s(\theta_s)$), as in Equation 7. The array response is a superposition of all wavenumbers, including both the incident wave response and the scattered waves. However, the wavenumber can be simply modified in the beamforming equations because the modification is just re-defining which wavenumbers are being considered (i.e. looking at the scattered region instead of the traditional region). The response measurement input to the beamform equation (y_n) is unchanged in the modified beamform equation and still contains information from all wavenumbers.

$$A(\theta) = \sum_{n=1}^{N} e^{i\left(k_s(\theta)-k_s(\theta_s)\right)x_n} \tag{7}$$

The calculated directivity using the scattered waves can be compared to the calculated directivity using traditional waves. If the calculated directivity is higher for scattered waves, the scattering in the array will enhance the directivity of the array.

III. Analysis of Bragg scattering directivity gains

The beamforming and DI calculations of scattered waves previously discussed were first applied to Bragg scattering in an array. The array's scattering was simulated using a high-order shear, closed form elastic plate model developed by Hull[22]. The model was used to predict the out of plane displacement response in a periodically ribbed array excited by a plane wave. The simulated array was modeled to be infinitely long and 0.01905 m thick, and included alternating 0.00635 m wide aluminum and 0.0508 m wide urethane, as shown in Figure 3. The urethane was chosen to have a modulus of elasticity of 1×10^8 Pa, a Poisson's ratio of 0.48, a density of 1070 kg/m^3, and a 25% damping. The aluminum was chosen to have a modulus of elasticity of 6.9×10^{10} Pa, a Poisson's ratio of 0.32, a density of 2700 kg/m^3, and a 0.5% damping. The damping values were chosen based on wave propagation measurements not discussed in this paper. The "measured" length of the simulated array was 1.82 meters, the total number of sensors (simulated points) was 288, and the excitation frequency was 1 kHz. The periodicity, a, was 0.05715 m. Any scattered Bragg wavenumber can be used in the scattered beamforming and DI calculations, however only the first positive scattered Bragg wave (n=1) was considered in this analysis. Higher order Bragg waves (n=2,3…) could be used, and would produce similar results if appropriately measured. Spatial aliasing becomes a concern with higher order, smaller wavelength portions of the signal, so for simplicity only the first Bragg wave is discussed. In addition, periodically placed transducers in the array could generate additional scattering. However, the effect of transducers on Bragg scattering in a periodically ribbed array was outside the scope of this paper.

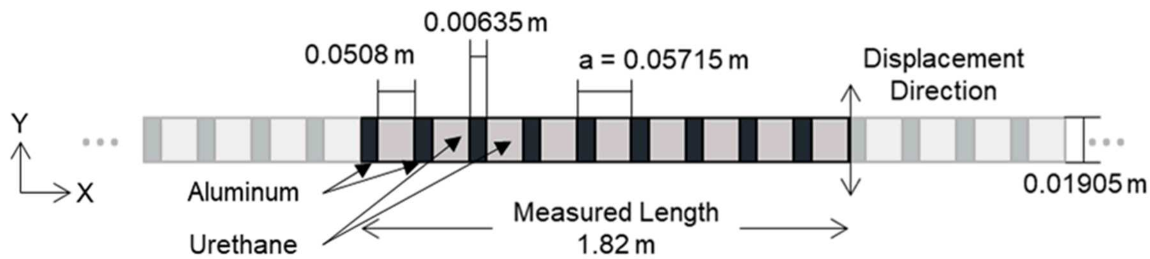

Fig. 3. Schematic of the Matlab model used to simulate Bragg scattering in a periodic array due to a plane wave excitation at □30° with the measured length and periodicity, a. The measurement sensors are not pictured.

The simulated Bragg array response was beamformed using Equation 2 and the traditional steering wavenumber ($k(\theta_s) = \omega/c \square \sin(\theta_s)$) was used to obtain the traditional beamform plot. Equation 3 and the first replicate Bragg scattered wavenumber ($k_s(\theta_s) = \omega/c \square \sin(\theta_s) + 2\pi/a$) was used to obtain the scattered wave beamform plot. The comparison between both beamforming methods is shown in Figure 4. Although some differences in the sidelobes occur, the main lobes of both beamform plots are identical in width, indicating that Bragg scattering with fixed periodicity does not improve array directivity.

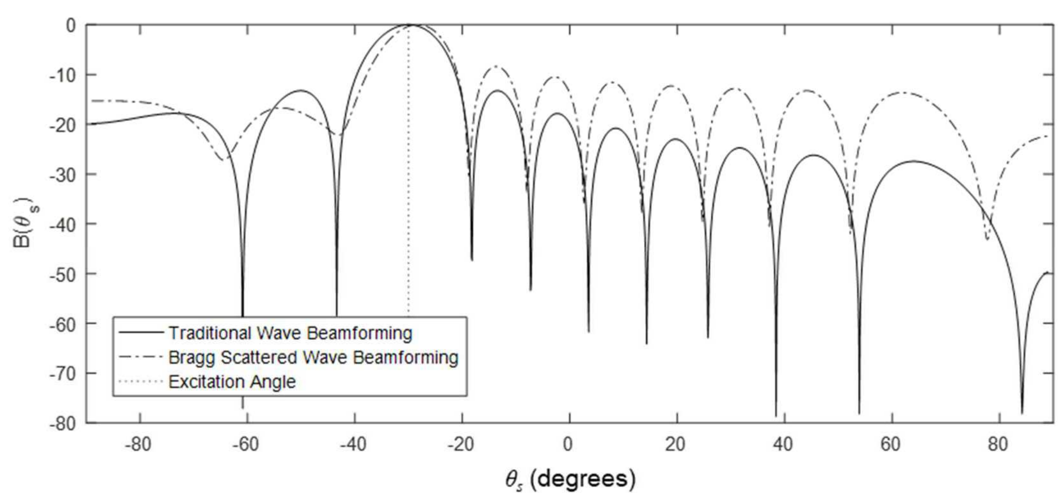

Fig. 4. Beamform plots of a 1 kHz plane wave excitation in air at □30° for a traditional array (solid line) and a periodic scattering array using the first Bragg replicate (dashed line).

Beamform plots are a good tool for the visualization of an array’s directivity, but the directivity index is required to understand if an array’s directivity is improved. The theoretical directivity of these Bragg scattered waves was calculated to identify why directivity was not enhanced. The angular response of the DI equation for scattered waves, given in Equation 5, was rewritten for Bragg scattering on an array with fixed periodicity, as shown in Equation 8. The additional Bragg scattered wave terms are shown in bold.

$$A(\theta) = \sum_{n=1}^{N} e^{i\left(\left(\frac{\omega}{c}\sin(\theta)+\boldsymbol{\frac{2\pi}{a}}\right)-\left(\frac{\omega}{c}\sin(\theta_s)+\boldsymbol{\frac{2\pi}{a}}\right)\right)x_n} \tag{8}$$

The additional wavenumber term for Bragg scattering is a constant dependent only on the periodicity of the array. When the DI is calculated for Bragg scattered waves, the additional Bragg term in the excitation scattered wavenumber cancels with the additional Bragg term in the steering scattered wavenumber, producing an array response term, and thus a DI, identical to the traditional DI. A plot of the identical DIs calculated using incident wave responses and scattered wave responses is shown in Figure 5. The increase in DI towards endfire (±90°) is expected based on the frequency and spacing used[23].

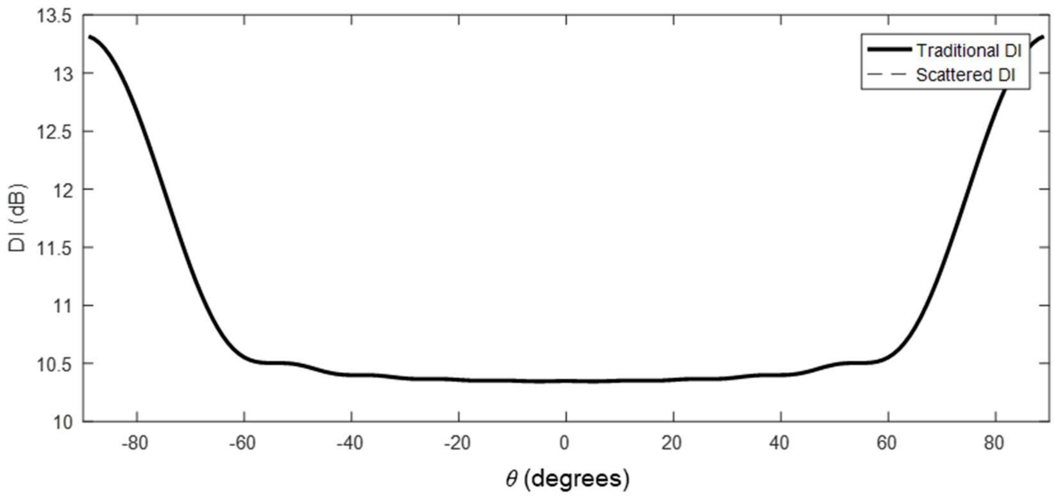

Fig. 5. DI values of a traditional array (solid line) and a periodic scattering array using the first Bragg replicate (dashed line) for a 1 kHz plane wave excitation incident at angles from □90° to 90°. The DI values are perfectly overlaid.

IV. Proposed scattering for directivity enhancement

Directivity enhancement was not achieved for Bragg scattering with fixed periodicity because the additional Bragg wavenumber term, $2\pi/a$, was constant for all incident angles and subsequently cancelled in the DI calculation. Therefore, scattering will only improve the directivity of an array if the scattering term is also a function of the incident angle of the excitation, preventing the additional scattering terms from cancelling and providing more information about the acoustic signal's location. Simply generating smaller wavelengths is not sufficient to improve directivity.

An analytical study was performed to confirm that Bragg scattering, as a function of excitation angle, increases an array's directivity. The Matlab model previously used to analyze Bragg scattering from a fixed periodic array was modified so that the periodicity of the array became a function of the incident angle, with the relationship between angle and spacing chosen to have the form of Equation 9. This form was chosen to avoid any singularities from a zero in the denominator, while keeping the maximum and minimum scattering terms close in value to reduce any aliasing effects in the beamforming process caused by wavenumber content above the Nyquist wavenumber.

The scattering term is then included in the wavenumber response as in Equation 10. The variable a_0 is a reference periodic spacing chosen to have a value of 0.05715 m for this analysis. Therefore, the scattered waves at 0° for angle-dependent scattering will have the same wavenumber values as the Bragg scattered wavenumbers at 0°, while negative excitation angles will excite smaller wavenumbers than conventional Bragg scattering and positive excitation angles will excite larger wavenumbers than conventional Bragg scattering.

$$a(\theta) = \frac{2a_0}{2 + \sin(\theta)} \tag{9}$$

$$k_n(\theta) = \frac{\omega}{c}\sin(\theta) + \frac{2\pi}{a(\theta)}n \tag{10}$$

A waterfall plot of wavenumber response as a function of excitation angle is shown for Bragg scattering in Figure 6a and the angle-dependent Bragg scattering (the proposed scattering) in Figure 6b. The Bragg scattering wavenumber-angle plots show that the spacing between wavenumber peaks is always constant, while the proposed scattering wavenumber spacing changes with incident angle.

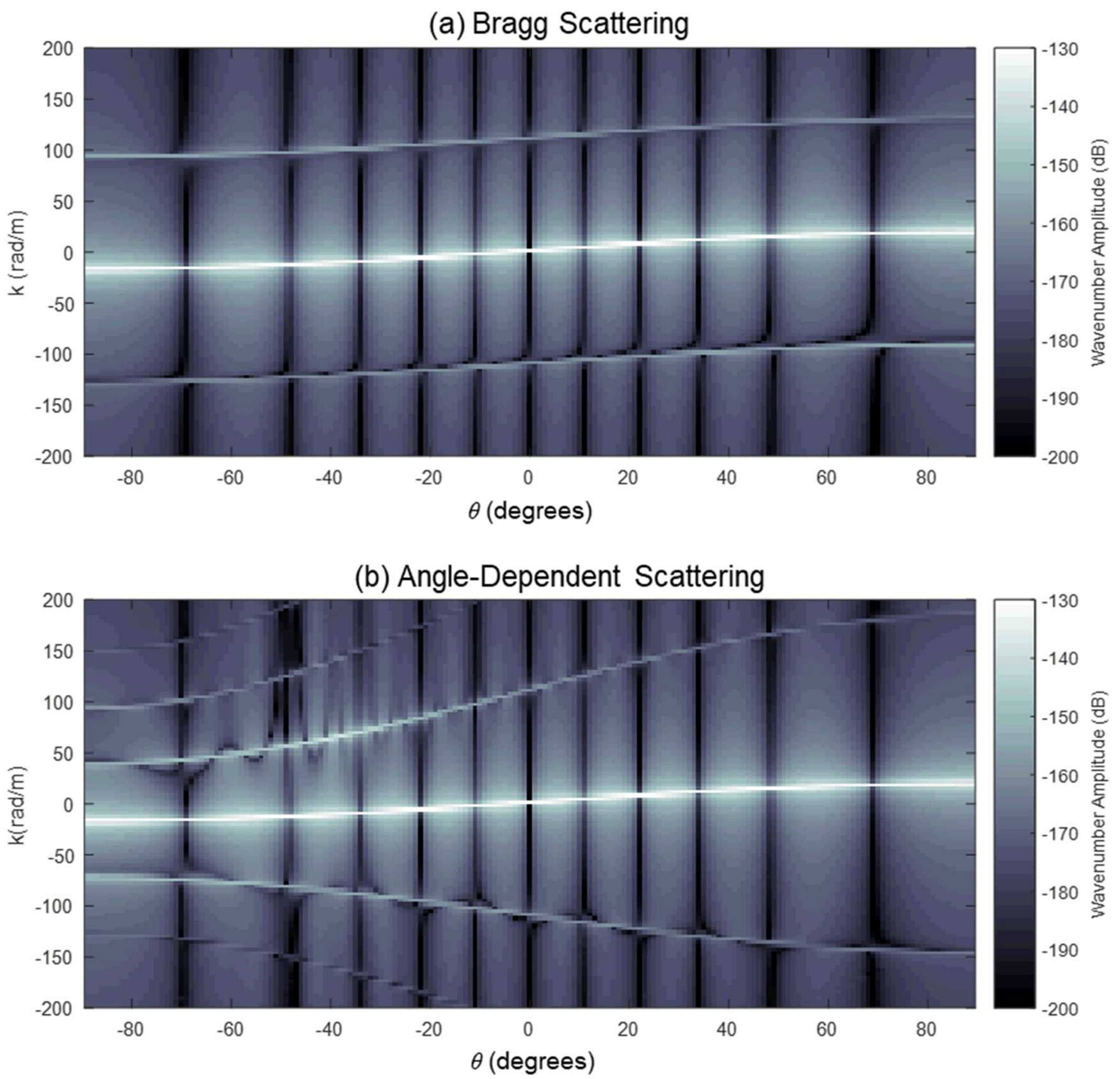

Fig. 6. Wavenumber-angle plots of a 1 kHz plane wave excitation at incident angles from −90° to 90° for (a) Bragg scattering and (b) the proposed angle-dependent scattering.

The simulated proposed scattering response was beamformed using Equations 1, 2, and 4, in which the wavenumber term in Equation 4 was written as Equation 10. The beamform plot generated from the proposed scattering response for the first scattered wave (n=1) is compared to the beamform plot from a traditional array of the same size in Figure 7. The scattered wave beamform plot produced a main lobe that is significantly narrower, without raising sidelobe levels, implying that directivity is enhanced.

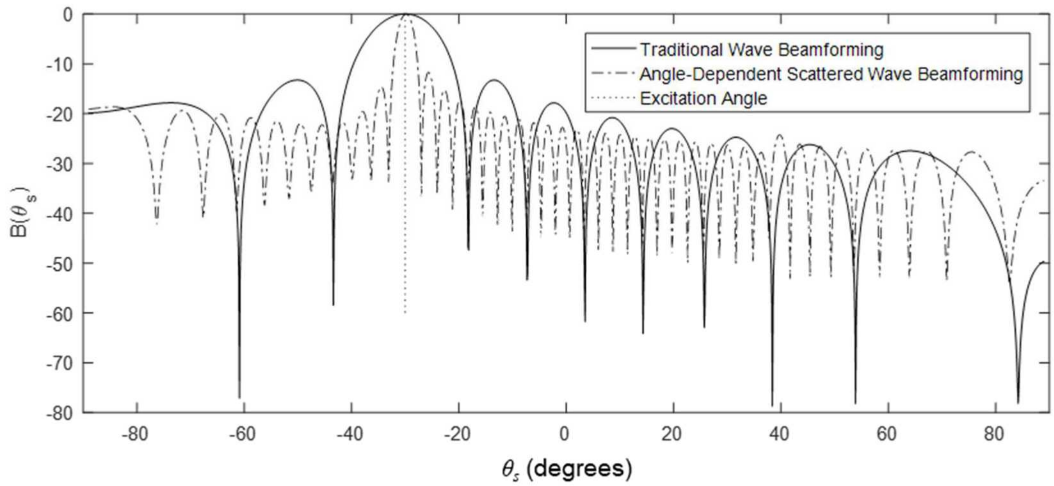

Fig. 7. Beamform plots of a 1 kHz plane wave excitation in air at □30° for a traditional array (solid line) and an array with the proposed scattering when n=1 (dashed line).

The directivity improvement through the use of scattered waves was quantified by calculating the DI for the proposed scattering. The angular response term for the first scattered wave (n=1) is shown in Equation 11, with the additional scattering terms shown in bold. The additional scattering terms, which do not cancel, can be rearranged into an additional exponent term, shown in bold in Equation 12. The angular response term, and therefore the DI, clearly increases through the use of the proposed scattered waves.

$$A(\theta) = \sum_{n=1}^{N} e^{i\left(\left(\frac{\omega}{c}\sin(\theta)+\frac{\boldsymbol{2\pi}}{\boldsymbol{a(\theta)}}\right)-\left(\frac{\omega}{c}\sin(\theta_s)+\frac{\boldsymbol{2\pi}}{\boldsymbol{a(\theta_s)}}\right)\right)x_n} \quad (11)$$

$$A(\theta) = \sum_{n=1}^{N} e^{i\left(\frac{\omega}{c}\sin(\theta) - \frac{\omega}{c}\sin(\theta_s)\right)x_n} \square\, \boldsymbol{e^{i\left(\frac{2\pi}{a(\theta)} - \frac{2\pi}{a(\theta_s)}\right)x_n}} \quad (12)$$

A comparison plot between the scattered wave DI and the DI of a traditional array of the same size is shown in Figure 8, and illustrates that DI was improved by 6 dB through the use of the proposed scattered waves.

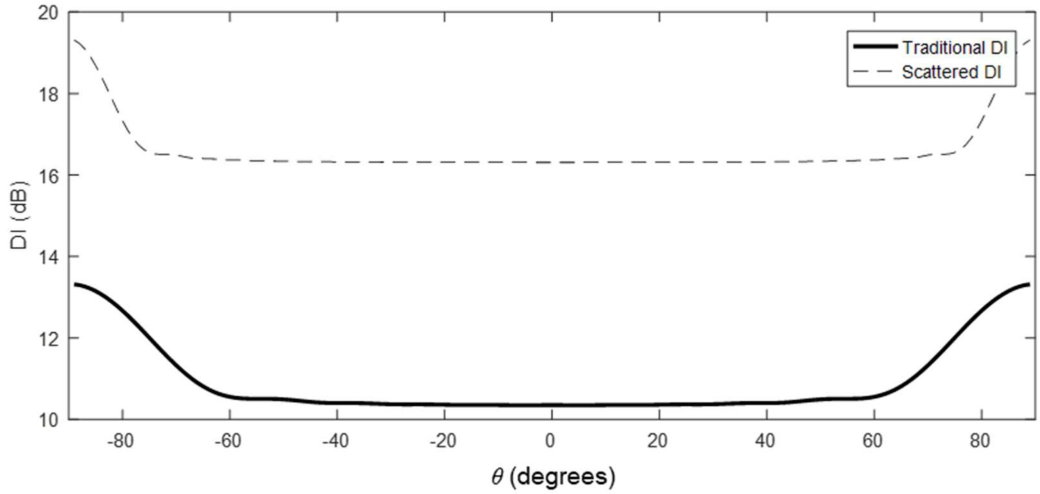

Fig. 8. DI values of a traditional array (solid line) and an array with the proposed scattering when n=1 (dashed line) for a 1 kHz plane wave excitation incident at angles from −90° to 90°.

The proposed scattering relationship has been shown to improve DI in an array without increasing the array size. If an array could be fabricated to generate the proposed scattering, then hull-mounted arrays could be significantly improved. However, the proposed scattering was achieved in this analysis by mathematically tying the rib spacing to the incident angle during the simulation, and no physical design was considered. To apply this relationship to an operational array, a new material will need to be designed and fabricated and it may be possible to do so by using additive manufacturing. One potential approach to create a material with the proposed scattering could be the fabrication of ribs that only appear for a narrow range of incident angles.

Overall, the findings in this paper have shown that nonhomogeneous arrays have the potential to achieve higher directivity with an equivalent aperture. In order to physically realize an array with the proposed scattering characteristics, further investigation into the material and design of nonhomogeneous arrays is required and serves as an attractive avenue of future research.

V. Conclusions

Array directivity improvements are primarily limited by size constraints. Wave scattering is a recently conceived method of directivity improvement that could avoid many of the drawbacks of previous directivity improvement methods, such as maneuverability limitations from the synthetic expansion method. However, previous proposed designs that implemented Bragg scattering on arrays with fixed periodicity were unsuccessful in directivity enhancement.

This paper proposes a scattering method applicable to plane wave signals incident on an array that exhibits angle-dependent scattering behavior. Traditional beamforming and DI equations were modified to consider scattered waves, and then used to study both conventional Bragg scattering and the proposed angle dependent Bragg scattering relationship. As expected, Bragg scattering with fixed periodicity did not achieve directivity improvements. However, the angle dependent scattering relationship proposed was shown to significantly narrow the main lobe of a beamform plot and increase DI by 6 dB for all excitation angles. The physical design of an array capable of producing such scattering is yet to be realized. The ability to design a material with the proposed scattering characteristics is expected to be plausible based on recent advances in additive manufacturing and considering the advancements recently observed in metamaterials.

Acknowledgements

The work presented herein was funded by the Naval Engineering Education Consortium (NEEC). Any opinions, findings, and conclusions or recommendations expressed in this material are those of the authors and do not necessarily reflect the views of the particular funding agency. Additionally, the authors would like to acknowledge Dr. Benjamin Cray, Dr. Andrew Hull, and Dr. Ivars Kirsteins for their consultation and advice.

*Sandia National Laboratories is a multimission laboratory managed and operated by National Technology & Engineering Solutions of Sandia, LLC, a wholly owned subsidiary of Honeywell International Inc., for the U.S. Department of Energy's National Nuclear Security Administration under contract DE-NA0003525.

This paper describes objective technical results and analysis. Any subjective views or opinions that might be expressed in the paper do not necessarily represent the views of the U.S. Department of Energy or the United States Government.

References

[1] Lord Rayleigh, "Investigations in optics, with special reference to the spectroscope," The London, Edinburgh, and Dublin Philosophical Magazine and Journal of Science, **8**(49), 261-274 (1879).

[2] L. R. Warren, "Hull-mounted sonar/ship design evolution and transition to low-frequency applications," IEEE Journal of Oceanic Engineering, **13**(4), 296-298 (1988).

[3] B. D. Van Veen and K. M. Buckley, "Beamforming: A versatile approach to spatial filtering," IEEE assp magazine, **5**(2), 4-24 (1988).

[4] J. Capon, "High-resolution frequency-wavenumber spectrum analysis," Proceedings of the IEEE, **57**(8), 1408-1418 (1969).

[5] C. D. Richmond, "Capon and bartlett beamforming: Threshold effect in direction-of-arrival estimation error and on the probability of resolution," Massachusetts Institute of Technology, Lexington, Lincoln Lab (2005).

[6] N.C. Yen and W. Carey, "Application of synthetic□aperture processing to towed□array data," The Journal of the Acoustical Society of America, **86**(2), 754-765 (1989).

[7] S. Stergiopoulos and E.J. Sullivan, "Extended towed array processing by an overlap correlator," The Journal of the Acoustical Society of America, **86**(1), 158-171 (1989).

[8] S. Stergiopoulos, "Optimum bearing resolution for a moving towed array and extension of its physical aperture," The Journal of the Acoustical Society of America, **87**(5), 2128-2140 (1990).

[9] B. A. Cray and G.R. Moss, "Enhanced directivity with array gratings," The Journal of the Acoustical Society of America, **136**(2), EL103-EL108 (2014).

[10] B. A. Cray, “Experimental verification of acoustic trace wavelength enhancement,” The Journal of the Acoustical Society of America, **138**(6), 3765-3772 (2015).

[11] P. A. Deymier, “Acoustic metamaterials and phononic crystals,” Springer Science & Business Media, 173, vii, (2013).

[12] B. C. Gupta and Z. Ye, “Theoretical analysis of the focusing of acoustic waves by two-dimensional sonic crystals,” Physical Review E, **67**(3), 036603 (2003).

[13] D. Richards and D. J. Pines, “Passive reduction of gear mesh vibration using a periodic drive shaft,” Journal of Sound and Vibration, **264**(2), 317-342 (2003).

[14] A. Khelif, A. Choujaa, S. Benchabane, B. Djafari-Rouhani, and V. Laude, “Guiding and bending of acoustic waves in highly confined phononic crystal waveguides,” Applied physics letters, **84**(22), 4400-4402 (2004).

[15] S. A. Cummer and D. Schurig, "One path to acoustic cloaking," New Journal of Physics, **9**(3), 45 (2007).

[16] M. Hussein, M. Leamy, and M. Ruzzene, “Dynamics of phononic materials and structures: Historical origins, recent progress, and future outlook,” Appl. Mech. Rev. 66, 040802 (2014).

[17] C. Elachi, “Waves in active and passive periodic structures: A review,” Proc. Inst. Electr. Electron. Eng. 64, 1666–1698 (1976).

[18] B. A. Cray, “Acoustic radiation from periodic and sectionally aperiodic rib□stiffened plates,” The Journal of the Acoustical Society of America, **95**(1), 256-264 (1994).

[19] B. A. Cray, “Erratum: Experimental verification of acoustic trace wavelength enhancement,” [J. Acoust. Soc. Am. **138**(6), 3765–3772 (2015)],” The Journal of the Acoustical Society of America, 140(5), 3738-3738 (2016).

[20] M. Brandstein and D. Ward, “Microphone arrays: signal processing techniques and applications,” Springer Science & Business Media, (2013).

[21] D. Lee and G. A. Leibiger, “Computation of Beam Patterns and Directivity Indices for Three-Dimensional Arrays with Arbitrary Element Spacings,” Naval Underwater Systems Center, New London, CT, No. NUSC-TR-4687 (1974).

[22] A. J. Hull, “A higher-order shear deformation model of a periodically sectioned plate,” Journal of Vibration and Acoustics, **138**(5), 051010 (2016).

[23] A. H. Nuttall and B. A. Cray, "Approximations to directivity for linear, planar, and volumetric apertures and arrays," IEEE journal of oceanic engineering, **26**(3), 383-398 (2001).